

# Effect of Swing Legs on Turning Motion of a Free-Falling Cat Robot

Jiaxuan Zhao

*School of Engineering Science*

*University of Science and Technology of China*

*Hefei, Anhui Province 230027, China*

*zjx123@mail.ustc.edu.cn*

Lu Li\*, Baolin Feng

*Institute of Advanced Manufacturing Technology*

*Hefei Institutes of Physical Science,*

*Chinese Academy of Sciences*

*Changzhou, Jiangsu Province 213164, China*

*{lli\* & blfeng}@iamt.ac.cn*

**Abstract** - Based on self-righting principle of a free-falling cat, a multi-rigid-body dynamic model of a cat robot is built with the consideration of swing legs and the relation between turning rate and swing angle of legs is got. Mechanical structure of the cat robot is designed and dynamics simulation is carried out to validate the theoretical analysis. Simulation results indicate that flip angle of the cat robot becomes larger with the increase of angle or angular velocity of swing legs. By contrast, the change of swing angle has more influence on flip angle of the cat robot. Adjusting angle and angular velocity of swing legs to suitable numerical values, energy consumption of turning motion can be reduced effectively.

**Index Terms** - Cat Robot, Swing Legs, Flip Angle, Energy Consumption, Modeling and Simulation.

## I. INTRODUCTION

It is well known that a cat can manage to right itself and land safely on its feet after being released upside-down from rest. This phenomenon is widely researched by scholars and provides an idea to solve the problem of safe landing of legged robot which falls from a height.

Explanation for the phenomenon can be traced back to the end of the 19th century. Guyou [1] researched the turning motion of a falling cat according to the law of angular momentum conservation. Loitsyansky [2] thought that the cat rotates tail rapidly and its body turns in reaction, but the experiment proved that a cat without tail can still restore its posture and perform safe landing. Kane and Scher [3] explained that the cat bends its torso but does not twist after falling from midair. They used two identical axial-symmetric rigid bodies to represent the front and back halves of the cat and established equations of motion. The numerical analysis result showed that motion of the model matched the photographic record of a falling cat very well.

In recent years, research on the problem of falling cats mainly includes the following aspects: motion control, mechanism analysis and prototype development. Takahashi [4] designed a quantum neural controller to solve the control problem that brings the falling cat from the initial to desired position. Nakano et al. [5] proposed a reinforcement learning approach to the control problem of a free-falling cat. Shields et al. [6] created a simplified model of a flipping cat robot and designed a simulation to demonstrate the mechanism of a

prototype. Kawamura [7] developed a robotic cat with two rectangular columns which are connected by a flexible spine and the robotic cat can right itself in midair. Liu [8] obtained the general characteristics of the turning motion of a free-falling cat. Zhong [9] explained that the free-falling cat can land on its feet from arbitrary posture. Ge and Guo [10] implemented the attitude planning of a free-falling cat and the optimal of control input by using spline approximation. Zhen et al. [11] applied the Udwadia-Kalaba approach to study the falling cat's movements. Yi and Ge [12] presented a hybrid optimal strategy to solve the attitude optimal control problem of a free-falling cat. Through observing a large number of high-speed photographs of the falling cat, we know that its legs swing regularly. However, most of researches about the falling cat do not consider the swing legs.

This paper mainly studies the influence of swing legs on the turning motion of a free-falling cat. First, we establish a simplified model of a robotic cat with the consideration of swing legs and analyses the relation between swing angle and turning rate. Next, we design the mechanical structure of the cat robot and a simulation environment has been constructed using ADAMS. Finally, we develop a cat robot with five servo actuators and then use a high-speed camera to shoot its turning motion.

## II. MODELING OF SYSTEM DYNAMICS

This section introduces characteristic of swing legs of the falling cat and proposes some assumptions in order to make the research convenient. Then we build a simplified model of a cat robot. According to the law of angular momentum conservation, we establish motion equations to analyse the effect of swing angle on moment of inertia and turning rate of the cat robot.

### A. Characteristic of Swing Legs

Photographs of a falling cat are shown in Fig. 1. Observing the pictures, we can know that when the cat is released from complete rest while upside-down, it first retracts forelegs and hindlegs close to the head and tail respectively and keep contractive posture for a while. Then the cat extends its forelegs and hindlegs to right itself completely. In order to simplify the inertia model of the cat robot, some assumptions are made as follows: 1) The swing of forelegs and hindlegs is axial-symmetric; 2) Two legs on each half body are assumed

to move as one; 3) The processes of leg retraction and extension cost the same time.

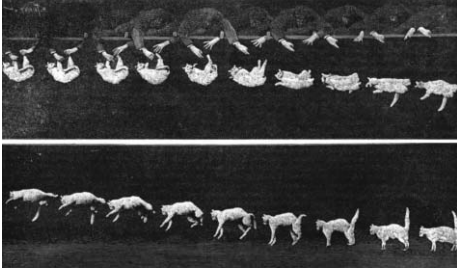


Fig. 1 Photographs of a falling cat [13].

### B. Analysis of Moments of Inertia

We use two kinds of circular columns whose size and mass distribution are identical to respectively represent torso and leg of the robotic cat model, as shown in Fig. 2. The front and back halves of its body are symmetric and the related parameters are marked in the multi-rigid-body dynamic model, as shown in Fig. 3. Torso is fixed with a constant angle  $2\theta$  between  $X_1$  and  $X_2$  axes.  $\theta$  is the bending angle of waist and its range is from  $0^\circ$  to  $90^\circ$ . Forelegs and hindlegs respectively swing around  $Y_1$  and  $Y_2$  axes.  $\beta$  is the swing angle of legs and its range is from  $0^\circ$  to  $90^\circ$ .

Since the robotic cat is released from complete rest, the model has no initial angular momentum and no external force is applied to it. The front and back halves of its body respectively rotate around  $X_1$  and  $X_2$  axes in the same direction with angular velocity  $w_s$ . According to the law of angular momentum conservation, the entirety of cat robot will rotate around the  $X_a$  axis which through two gravity centers,  $G_1$  and  $G_2$ , of the front and back halves of the cat robot in the opposite direction with the angular velocity  $w$ .

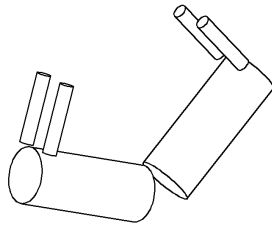


Fig. 2 Robotic cat model.

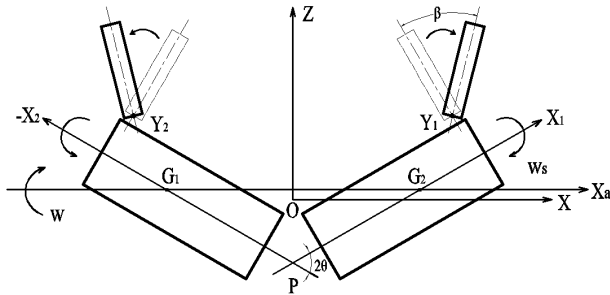


Fig. 3 The multi-rigid-body dynamic model.

Based on the above analysis, we can get the following equation:

$$2Iw + 2I_s w_s \cos \theta = 0 \quad (1)$$

where  $I$  is moment of inertia of each half body related to  $X_a$  axis,  $I_s$  is moment of inertia of each half body respectively related to  $X_1$  and  $X_2$  axes. From (1), we can get

$$w_s = -\frac{I}{I_s \cos \theta} w \quad (2)$$

Turning rate of the cat robot is defined by (3) [14]:

$$R_t = 1 + \frac{w}{w_s} = 1 - \frac{I_s}{I} \cos \theta \quad (3)$$

From (3), we know that the next step is to solve the expression of  $I_s$  and  $I$ .  $I_s$  is expressed in (4),

$$I_s = I_{T1} + I_{L1} \quad (4)$$

where  $I_{T1}$  is moment of inertia of front half of torso related to  $X_1$  axis,  $I_{L1}$  is moment of inertia of forelegs related to  $X_1$  axis. The expressions of  $I_{T1}$  and  $I_{L1}$  are as follows:

$$I_{T1} = \frac{1}{2} MR^2 \quad (5)$$

where  $M$  is the mass of the front half of torso,  $R$  is the radius of the front half of torso.  $I_{L1}$  is expressed in (6) [15],

$$I_{L1} = \frac{1}{2} mr^2 + \frac{1}{12} m \sin^2 \left( \frac{\pi}{2} - \beta \right) (h^2 - 3r^2) + md_1^2 \quad (6)$$

where  $m$  is the mass of forelegs,  $r$  is the radius of the leg,  $h$  is the leg length,  $d_1$  is the distance between the centre of gravity of the leg and  $X_1$  axis. The expression of  $d_1$  is as follows:

$$d_1 = \sqrt{\left[ R + r + \frac{1}{2} h \sin \left( \frac{\pi}{2} - \beta \right) \right]^2 + (R - r)^2} \quad (7)$$

$I$  is expressed in (8),

$$I = I_T + I_L \quad (8)$$

where  $I_T$  is moment of inertia of the front half of torso related to  $X_a$  axis,  $I_L$  is moment of inertia of forelegs related to  $X_a$  axis. The expressions of  $I_T$  and  $I_L$  are as follows [15]:

$$I_T = \frac{1}{2} MR^2 + \frac{1}{12} M \sin^2 \theta (H^2 - 3R^2) + M \left( \frac{mL_z}{M + m} \right)^2 \quad (9)$$

where  $H$  is the length of the front half of torso,  $L_z$  is the center of gravity of the leg corresponds to the coordinate of the  $Z$  axis.

$$L_z = c + \frac{1}{2} h \sin \left( \frac{\pi}{2} - \beta + \theta \right) \quad (10)$$

where  $c$  is the distance between  $Y_1$  axis and  $X$  axis. Its expression is as follows:

$$c = \frac{r + 2R}{\cos \theta} + \left[ \frac{1}{2} H - \frac{R}{\tan \theta} - (r + 2R) \tan \theta - r \right] \sin \theta \quad (11)$$

$$I_L = \frac{1}{2} mr^2 + \frac{1}{12} m \sin^2 \left( \frac{\pi}{2} - \beta + \theta \right) (h^2 - 3r^2) + md_a^2 \quad (12)$$

where  $d_a$  is the distance between the centre of gravity of the leg and  $X_a$  axis. Its expression is as follows:

$$d_a = \sqrt{\left( L_z - \frac{mL_z}{M + m} \right)^2 + (R - r)^2} \quad (13)$$

We assign numerical values to parameters except  $\beta$  in order to simplify expression of  $I_s$  and  $I$ . Where  $M=2\text{kg}$ ,  $m=0.5\text{kg}$ ,  $R=40\text{mm}$ ,  $r=15\text{mm}$ ,  $H=150\text{mm}$ ,  $h=100\text{mm}$ ,  $\theta=30^\circ$ . The numerical values given for the parameters are based on the current model of the cat robot, then we can obtain:

$$I_s = (1.6 \cos^2 \beta + 2.8 \cos \beta + 3.5) \times 10^{-3} \quad (14)$$

$$I = [1.4 \cos^2(\frac{\pi}{6} - \beta) + 3.1 \cos(\frac{\pi}{6} - \beta) + 5.1] \times 10^{-3} \quad (15)$$

Plugging (13) and (14) into (3), we get the relation between turning rate and swing angle of legs:

$$R_t = 1 - \frac{1.6 \cos^2 \beta + 2.8 \cos \beta + 3.5}{1.4 \cos^2(\frac{\pi}{6} - \beta) + 3.1 \cos(\frac{\pi}{6} - \beta) + 5.1} \times \frac{\sqrt{3}}{2} \quad (16)$$

Fig. 4 shows the relation between turning rate and swing angle. Fig. 5 shows the effect of swing angle on  $I$  and  $I_s$ . From Fig. 4, we can see that the turning rate becomes larger with the increase of swing angle. From Fig. 5, we know that  $I_s$  becomes smaller with the increase of swing angle, but  $I$  increases first and then decreases as a result of the bending angle of waist. Since the ratio of  $I_s$  to  $I$  becomes smaller with the increase of swing angle, so according to (3) we can know that the turning rate becomes larger when the bending angle is constant.

### III. DYNAMICS SIMULATION

In this section, we design a 3D modeling of a cat robot and then use ADAMS to analyse the influence of angle and angular velocity of swing legs on flip angle and energy consumption of the turning motion of the cat robot. The simulation results also provide reference data for the final prototype experiment.

#### A. Structure Design of a Cat Robot

We design the structure of a cat robot which consists of the waist, torso and legs, as shown in Fig. 6. The material of each part is resin whose density is  $1.1 \text{ g/cm}^3$ . The motion of each part is driven by a servo actuator whose mass is  $52\text{g}$ . Servo actuator 5 and 9 separately control the rotation of the front and back halves of the cat robot. Servo actuator 7 adjusts the bending angle of the waist. Servo actuator 2 and 3 separately control the swing of forelegs and hindlegs which are fixed on the gear shafts. The transmission ratio is 0.607.

#### B. Simulation Analysis

In order to simplify the analysis, we assume that the motion of each part is uniform. We define the drop height of the cat robot is  $2\text{m}$  and its bending angle of waist is  $30^\circ$ , so the fall time is  $0.64\text{s}$ . We set the time of turning motion is the initial  $0.5\text{s}$ , so the angular velocity of servo actuator 5 and 9 is  $12.56\text{rad/s}$ . Then the cat robot flattens its waist in the remaining  $0.14\text{s}$ , so the angular velocity of servo actuator 7 is  $7.48\text{rad/s}$ . In the simulation environment, we set the end time is  $0.64\text{s}$  and steps are 500.

##### 1) Effect of Swing Angle of Legs on Turning Motion

According to the principle of single variable, we set the angular velocity of swing legs is constant and its numerical

value is  $8\text{rad/s}$ , we can obtain the angular velocity of servo actuator 2 and 3 is  $4.86\text{rad/s}$ . The range of swing angle of simulation input is from  $0^\circ$  to  $90^\circ$  and the interval angle is  $10^\circ$ . Fig. 7 shows the relation between flip angle and swing angle. It can be seen from the figure that swing angle goes from  $0^\circ$  to  $90^\circ$ , flip angle of the cat robot goes from  $102^\circ$  to  $210^\circ$ .

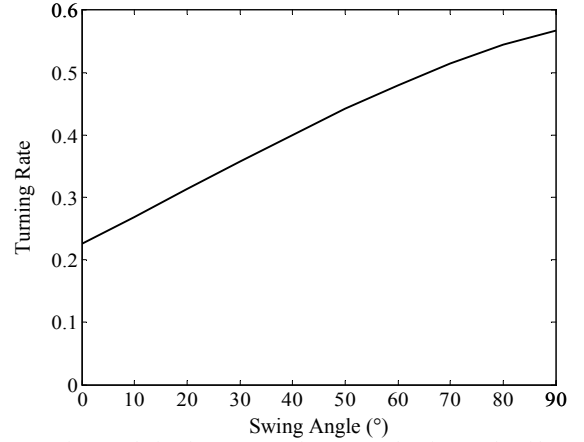


Fig. 4 Relation between turning rate and swing angle of legs.

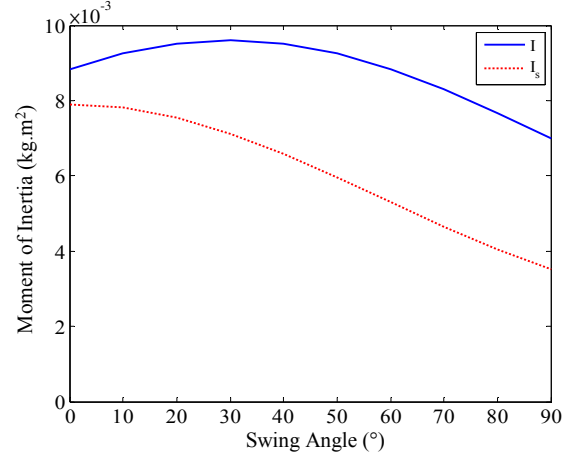


Fig. 5 The effect of swing angle of legs on moment of inertia  $I$  and  $I_s$ .

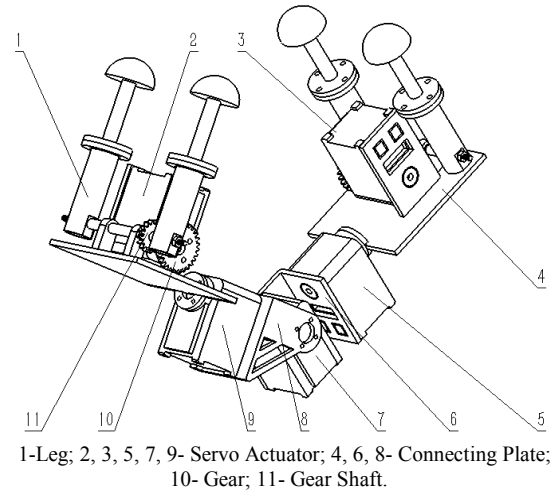


Fig. 6 3D modeling of the cat robot.

So the simulation result is consistent with the conclusion from previous theoretic analysis. In all angles of simulation input, the cat robot has the minimum turning error when the swing angle of legs is  $60^\circ$ . The corresponding flip angle of the cat robot is  $184^\circ$  and the righting process is shown in Fig. 8.

The total energy consumption  $W$  of turning motion of the cat robot is composed of two parts: the energy consumption  $W_1$  of the rotation of the front and back halves of the cat robot and the energy consumption  $W_2$  of the swing of forelegs and hindlegs. The expressions of  $W_1$  and  $W_2$  are as follows:

$$W_1 = 2w_1 \int_0^{0.5} T_1 dt \quad (17)$$

where  $w_1$  and  $T_1$  are angular velocity and torque of servo actuator 5 and 9, respectively.

$$W_2 = 2w_2 \int_0^{0.5} T_2 dt \quad (18)$$

where  $w_2$  and  $T_2$  are angular velocity and torque of servo actuator 2 and 3, respectively. The variation curves of  $T_1$  and  $T_2$  with time under different swing angles are shown in Fig. 9 and Fig. 10, respectively.

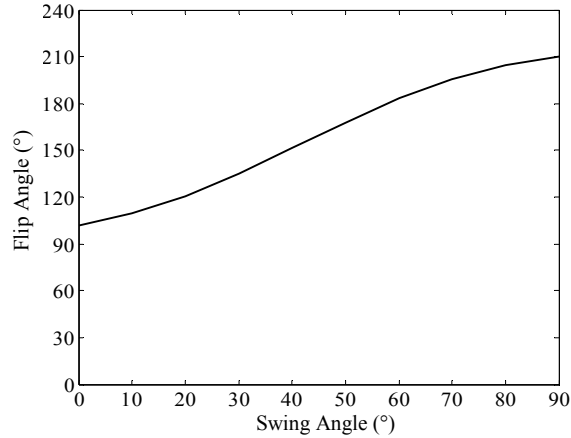


Fig. 7 Relation between flip angle of the cat robot and swing angle of legs.



Fig. 8 Righting process of the cat robot.

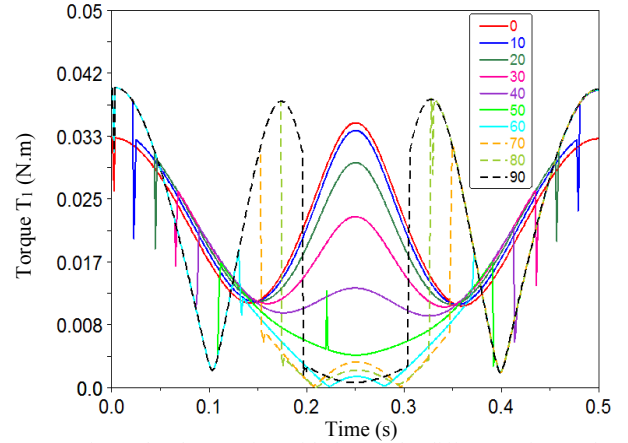


Fig. 9 The change of  $T_1$  with time under different swing angles.

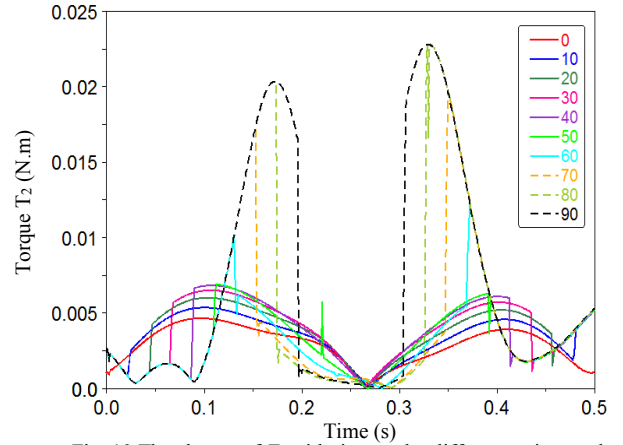


Fig. 10 The change of  $T_2$  with time under different swing angles.

The integral value of the torque curve is multiplied with the corresponding angular velocity, then the each part and total energy consumption can be obtained, as shown in Fig. 11.

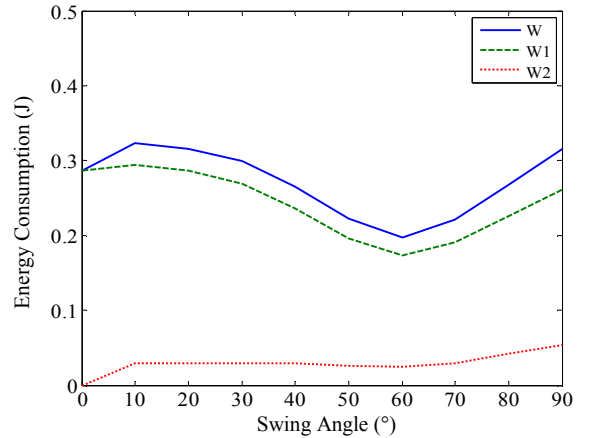


Fig. 11 Effect of swing angle of legs on each part and total energy consumption.

It's easy to see that the swing legs can generate energy consumption, but they are beneficial to reduce the energy consumption of rotation of the front and back halves of the cat robot. In all angles of simulation input, the optimal swing

angle value corresponding to the lowest energy consumption is  $60^\circ$ . The total energy consumption of the cat robot under this swing angle is reduced by 31.1% compared with the cat robot without legs swinging.

## 2) Effect of Angular Velocity of Swing legs on Turning Motion

According to the principle of the single variable, we set the swing angle of legs is constant and angle value is  $60^\circ$ . The numerical values of angular velocity are as follows: 8rad/s, 12rad/s, 16rad/s, 20rad/s. Fig. 12 shows the relation between flip angle and angular velocity. When the angular velocity goes from 8rad/s to 20rad/s, flip angle goes from  $183^\circ$  to  $184.2^\circ$ . So increasing the angular velocity can also improve the turning rate, but the influence is very small. The variation curves of  $T_1$  and  $T_2$  with time under different angular velocities are shown in Fig. 13 and Fig. 14, respectively.

Similarly, we can obtain the variation curves of each part and total energy consumption, as shown in Fig. 15. It can be seen from the figure that each part and total energy consumption become larger with the increase of the angular velocity. The increase of energy consumption of swing legs is particularly evident. So in order to keep the total energy consumption of turning motion of the cat robot at a lower level, the angular velocity of swing legs should be small under the premise that the legs can finish the swing within the stipulated time.

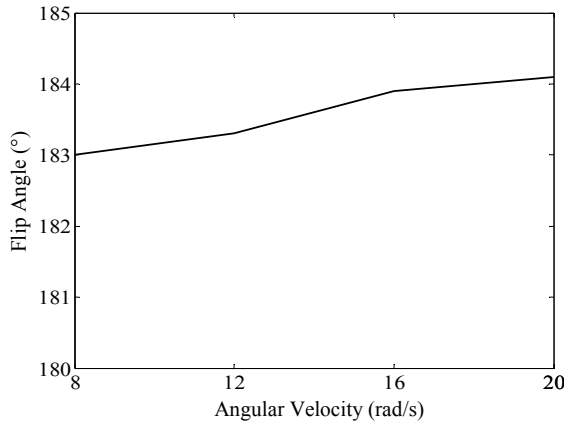


Fig. 12 Relation between flip angle of the cat robot and angular velocity of swing legs.

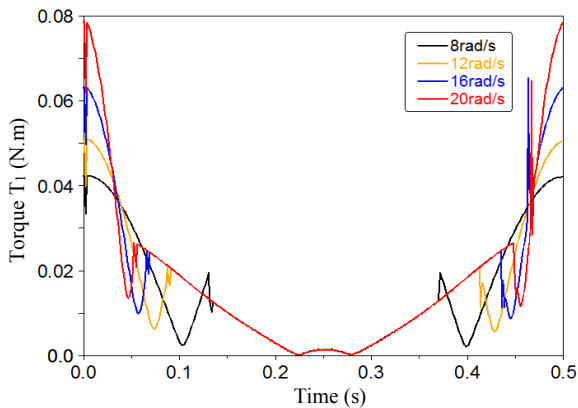


Fig.13 The change of  $T_1$  with time under different angular velocities.

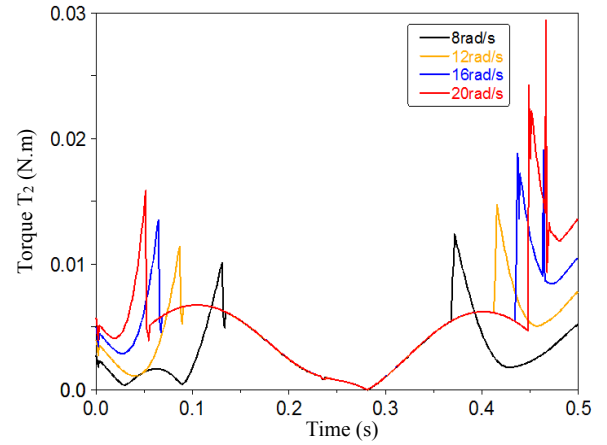


Fig. 14 The change of  $T_2$  with time under different angular velocities.

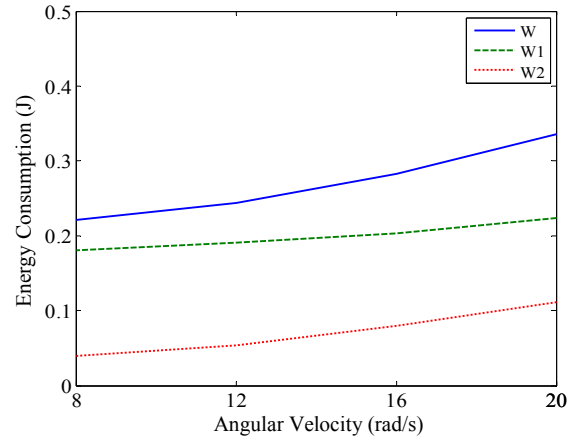


Fig. 15 Effect of angular velocity of swing legs on each part and total energy consumption.

Fig. 16 and Fig. 17 respectively show the variations of flip angle and energy consumption when angle and angular velocity of swing legs change together. We can see from the two figures that adjusting angle and angular velocity of swing legs to suitable numerical values, not only can the flip angle be improved, but also the energy consumption can be reduced.

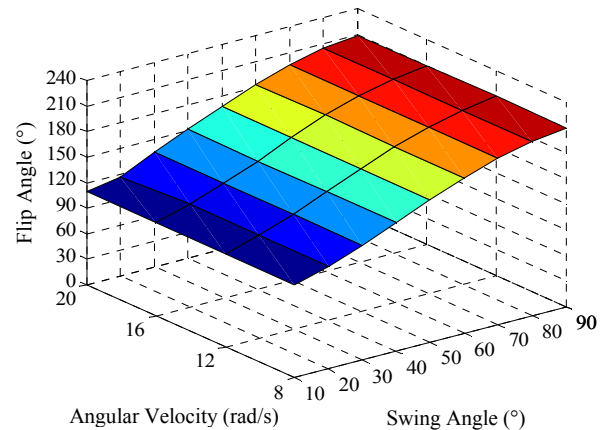


Fig. 16 Effect of angle and angular velocity of swing legs on flip angle of the cat robot.

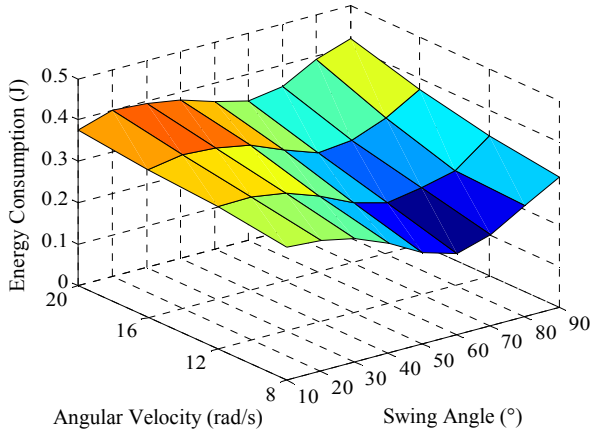


Fig. 17 Effect of angle and angular velocity of swing legs on total energy consumption.

In order to indicate whether the time of turning motion will change the influence of swing legs on flip angle and energy consumption of the cat robot, we do the same simulation when the time of turning motion is 0.4s, 0.6s, 0.8s and 1s, respectively. The results show that the change laws of flip angle and energy consumption with different swing angles and angular velocities are the same under different time of turning motion. In all angles of simulation input, the optimal swing angle value remains unchanged, but the energy of consumption of the cat robot will be reduced with the increase of time of turning motion. The longer time of turning motion means that the cat robot will fall from a higher height and it needs to withstand a greater impact from contact surface.

#### IV. EXPERIMENT

Experimental prototype of the cat robot is shown in Fig. 18 and the control of each servo actuator is based on STM32 MCU. The experiment of turning motion of the cat robot is carried out by suspended method. The experimental process is recorded by a high-speed camera.

The values of motion parameters of the prototype are set as follows: bending angle of waist  $\theta$  is  $30^\circ$ , swing angle of legs  $\beta$  is  $60^\circ$ , angular velocity of swing legs is  $8\text{rad/s}$ , the total time is  $0.64\text{s}$ , where the time of turning motion is the initial  $0.5\text{s}$ , then the cat robot unbends its waist in the remaining  $0.14\text{s}$ . The angular velocity of servo actuator 5 and 9 is  $12.56\text{rad/s}$ , the angular velocity of servo actuator 7 is  $7.48\text{rad/s}$ , the angular velocity of servo actuator 2 and 3 is  $4.86\text{rad/s}$ .

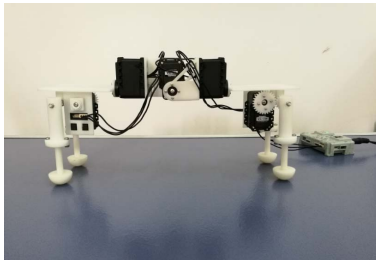


Fig. 18 Experimental prototype of the cat robot.

The comparison between simulation result and the actual righting process of the cat robot prototype is shown in Fig. 19. In order to facilitate the comparison, the experimental photos are rotated 90 degrees clockwise. It can be seen from the pictures that the actual righting process of the prototype is in good agreement with simulation result.

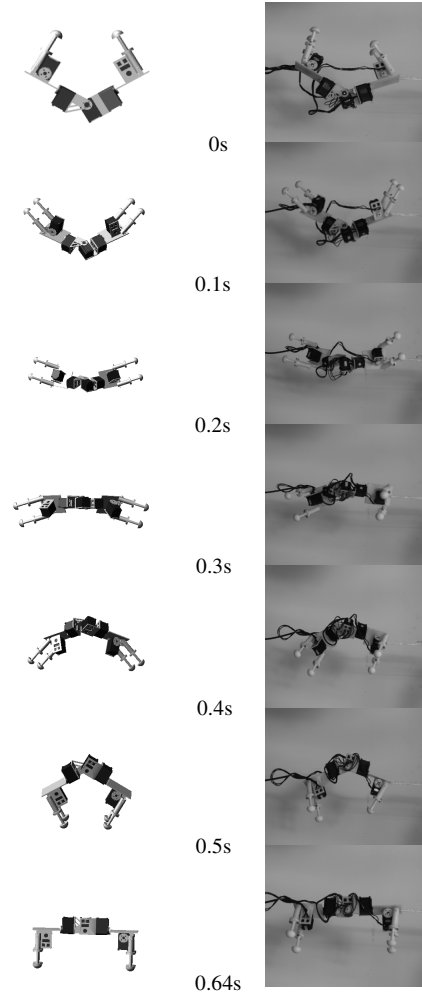


Fig. 19 The comparison between simulation result and actual righting process of the cat robot prototype.

#### V. CONCLUSIONS AND FUTURE WORK

In this paper, a multi-rigid-body dynamic model of a free-falling cat robot is built with the consideration of swing legs. Through theoretical analysis and calculation, we come to the conclusion that turning rate of the cat robot will increase when swing angle of legs becomes large. We design a 3D modeling of a cat robot and then use ADAMS to carry out dynamic simulation. The simulation results show that adjusting the angle and angular velocity of the swing legs to suitable numerical values, not only can the flip angle be improved, but also the energy consumption can be reduced effectively. A cat robot prototype is developed and the turning motion of the prototype is implemented successfully in the experiment.

For future work, we will add gyroscopes and pressure sensors to the cat robot prototype in order to get the accurate data of turning motion and indicate the influence of landing attitude, elastic leg and flexible waist on landing stability, finally present mechanisms and implementation methods of safe landing of quadruped robots.

#### ACKNOWLEDGMENT

This project is supported by the National Natural Science Foundation of China (Grant No. 51405470).

#### REFERENCES

- [1] E. Guyou, *Note Sur Les Approximations Numeriques*, Montana: Kessinger Publishing, 1891.
- [2] A. I. Loitsyansky, *Theoretical Mechanics*, Moscow: Saint Petersburg, 1953.
- [3] T. R. Kane and M. P. Scher, "A dynamical explanation of the falling cat phenomenon," *Int. J. of Solids and Structures*, vol. 5, no. 7, pp. 663-670, 1969.
- [4] K. Takahashi, "Remarks on motion control of nonholonomic system (falling cat) by using a quantum neural controller," *International Conference on Intelligent Systems Design and Applications*, pp. 961-966, 2012.
- [5] D. Nakano, S.-I. Maeda and S. Ishii, "Control of a free-falling cat by policy-based reinforcement learning," *International Conference on Artificial Neural Networks*, pp. 116-123, 2012.
- [6] B. Shields, W. S. P. Robertson, N. Redmond, R. Jobson, R. Visser, Z. Prime and B. Cazzolato, "Falling cat robot lands on its feet," *Proceedings of the Australasian Conference on Robotics and Automation*, pp. 74-82, 2013.
- [7] T. Kawamura, "Understanding of falling cat phenomenon and realization by robot," *Journal of Robotics and Mechatronics*, vol. 26, no. 6, pp. 685-690, 2014.
- [8] Y. Liu, "On the turning motion of a free-falling cat," *Acta Mechanica Sinica*, vol. 14, no. 4, pp. 388-393, 1982.
- [9] F. Zhong, "A two-rigid-body model of the free-falling cat," *Acta Mechanica Sinica*, vol. 17, no. 1, pp. 72-78, 1985.
- [10] X. Ge and Z. Guo, "Nonholonomic motion planning for a free-falling cat using spline approximation," *Science China: Physics, Mechanics and Astronomy*, vol. 55, no. 11, pp. 2100-2105, 2012.
- [11] S. Zhen, K. Huang, H. Zhao and Y.-H. Chen, "Why can a free-falling cat always manage to land safely on its feet?" *Nonlinear Dynamics*, vol. 79, no. 4, pp. 2237-2250, 2015.
- [12] Z. Yi and X. Ge, "The attitude optimal control with a hybrid optimal strategy for a free-falling cat," *Chinese Journal of Theoretical and Applied Mechanics*, vol. 48, no. 6, pp. 1390-1397, 2016.
- [13] E. J. Marey, "Falling cat," [https://en.wikipedia.org/wiki/Falling\\_Cat](https://en.wikipedia.org/wiki/Falling_Cat).
- [14] K. Yamafuji, T. Kobayashi and T. Kawamura, "Elucidation of twisting motion of a falling cat and its realization by a robot," *Int. J. of the Robotics Society of Japan*, vol. 10, no. 5, pp. 92-98, 1992.
- [15] K. Yang, "The formula of moment of inertia of homogeneous cylinder type of rigid body about any axis," *Mechanics in Engineering*, no. 5, pp. 53-54, 1983.